ACS Sustainable Chemistry & Engineering

Research Article

pubs.acs.org/journal/ascecg

Performance Enhancement with a Hydrophilic Self-Immobilized Redox Mediator Modified Anode in *Chlorella vulgaris*-based Microbial Solar Cell

Keliang Pan and Peijiang Zhou*

School of Resource and Environmental Science, Hubei Biomass-Resource Chemistry and Environmental Biotechnology Key Laboratory, Wuhan University, 129#, Luoyu Road, Wuhan 430079, People's Republic of China

Supporting Information

ABSTRACT: In this study, a new approach to improving the performance of a *Chlorella vulgaris*-based microbial solar cell (MSC) by using a riboflavinyl-salicylaldehyde-4-aminosalicylic-1-tetracarboxylate ester (RSA) modified carbon rod anode was reported. It has strong hydrophilicity but can be easily soluble in organic solvents rather than water and can be attached to the surface of a plain carbon rod without using any carrier. The single-chamber MSC operated with this RSA modified anode and a cupric hexacyanoferrate modified cathode achieved a maximum power density of 0.847 W/m^2, which was 7 times higher than that obtained from the MSC equipped with an unmodified anode. The scanning electron microscopy (SEM) results indicated that there was no biofilm formed on the anode surface. Charge transfer was facilitated only by RSA modification.

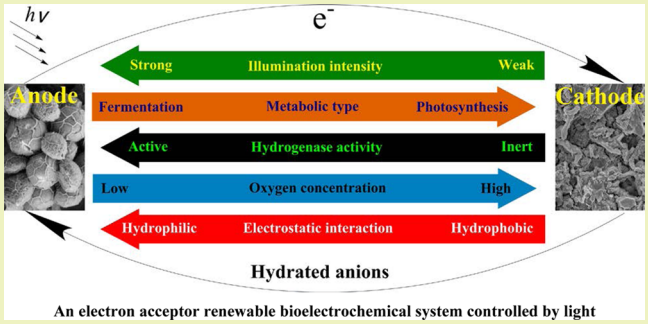

An electron acceptor renewable bioelectrochemical system controlled by light

KEYWORDS: *Microbial solar cells, Redox mediator, Riboflavin, Hydrophilic, Chlorella vulgaris*

INTRODUCTION

As a promising energy technology, microbial fuel cells (MFCs) have been developed extensively. Although it is difficult to utilize them on a large-scale at present, the working mechanisms of MFCs have been detailed and studied in depth. A suitable redox mediator (RM), the most important part of electronic transmission, is critical in the constructing of MFCs. Admittedly, though the external soluble redox mediators have excellent performance, they have the disadvantage of easy loss. Self-generated redox mediators or nanowire from microbes can solve the above-mentioned problem to a certain extent, but they increase the limitations of selections of microorganisms greatly.[1,2] For these reasons, the immobilization of redox mediators on the surface of an electrode proves to be a useful method to enhance power output and reduce the loss of catalysts. In fact, the techniques of immobilization of redox mediators have been studied extensively. Porphyrins,[3] phthalocyanine,[4] anthraquinone-2,6-disulfonic disodium salt,[5] ethylenediamine[6] or pyrolyzed iron ethylenediaminetetraacetic acid,[7] metal oxides[8] and polyoxometalate[9] are commonly used modifiers. For the cathode modifications, strong oxidants such as manganese dioxide,[10] percarbonate,[11] potassium ferricyanide,[12] persulfate[13] and permanganate[14] are the most commonly used compounds. What all these techniques have in common is that the RMs are adsorbed or embedded in certain carriers such as polyaniline,[15] polypyrrole and polyethylenimine[16] and then the carriers are attached to the surface of electrodes like amorphous carbon,[17] graphite,[18] carbon nanotube,[19] graphene oxide,[20] tungsten[15,21] and even the natural loofah sponge.[22] Among these carriers, the conductive polymers have excellent performance. They can not only maintain the stability of RMs but also provide hydrophobic cavities for the growth of microorganisms. However, most carriers themselves do not have the reversible nature of electrons gain and loss. On the other hand, the inherent properties of RM are not changed by immobilization. The soluble catalysts will still be lost and the cost might increase.[23−25]

Synthesizing a water-insoluble flavin derivative and immobilizing it on the plain carbon rod surface is the strategy to solve the above-mentioned problems. This modifier of the anode material is a riboflavinyl-salicylaldehyde-4-aminosalicylic-1-tetracarboxylate ester (RSA). This compound has the function with both the RM and the carrier. To evaluate the performance of this RM, a *Chlorella vulgaris* (*C. vulgaris*)-based microbial solar cell (MSC) was established. Because *C. vulgaris* can utilize light energy[26] to maintain its life activities and synthesize cell organic molecules,[27] it provides conveniences for the research of self-sustained equipment, which is the new focus of the energy and environmental field.[28] Although *C. vulgaris* has the ability to form biofilms,[29] this process might take a long time. This makes the required lengths of time of start-up period

Received: February 27, 2015
Revised: July 20, 2015
Published: August 18, 2015

DOI: 10.1021/acssuschemeng.5b00151
ACS Sustainable Chem. Eng. 2015, 3, 1974−1981

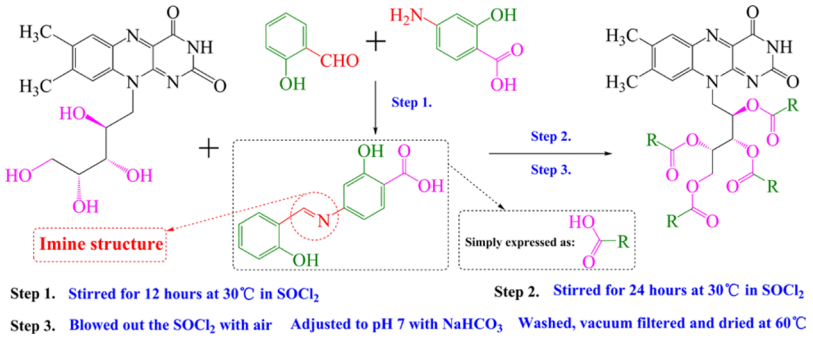

Figure 1. Synthetic route of RSA.

increase. The algal cells in this study were suspended in solution and would not form biofilm. In this case, *C. vulgaris* would cause almost no harm to the surface of the electrode. This is also the reason and advantage for the requirement of an immobilized RM. Although *C. vulgaris* is a light autotrophic microorganism, organic carbon sources were still added to evaluate the performance of MSCs in this study. These facilitated the rapid assessment of RM performance and accurate calculation of Coulombic efficiency (CE). A set of control experiments that contained no RM, used anthraquinone (AQ, a hydrophobic RM) modified anode or added riboflavin (RF, a water-soluble RM) were also conducted. Although algal cells could produce organics through photosynthesis, all these systems have the same background values. The errors of producing organics by *C. vulgaris* can be deducted by the blank tests. The property of RSA, the surface morphology of anode and the performance of MSCs were also examined.

EXPERIMENTAL SECTION

Microbial Growth and Inoculum Preparation. *C. vulgaris* (FACHB-1227) was obtained from Freshwater Algae Culture Collection of the Institute of Hydrobiology (FACHB-collection, Institute of Hydrobiology, Chinese Academy of Sciences, China). It was incubated anaerobically at 30 ± 2 °C in a liquid medium that contained 5 g of CH_3COONa, 1 g of NH_4Cl, 1 g of KNO_3, 0.6 g of KH_2PO_4, 0.4 g of K_2HPO_4, 0.1 g of $CaCl_2$, 0.1 g of $MgSO_4$ and 1 mL of trace elements solution (which contained 2.86 g of H_3BO_3, 1.81 g of $MnCl_2{\cdot}4H_2O$, 0.222 g of $ZnSO_4{\cdot}7H_2O$, 0.391 g of $Na_2MnO_4{\cdot}2H_2O$, 0.079 g of $CuSO_4{\cdot}5H_2O$ and 0.049 g of $Co(NO_3)_2{\cdot}6H_2O$ per liter) per liter for 3 days. The medium was sealed in a transparent common glass sample vial. Because the original system did not undergo deaeration, the device still contained a certain concentration of O_2. In a sealed culture of *C. vulgaris*, the photosynthetic O_2 evolution rate dropped below the rate of respiratory O_2 consumption by increasing the illumination intensity (3000 lx, fluorescent lamp). Thus, an anaerobic microenvironment was produced.[30] Methylene blue (MB), which is colorless in reducing atmosphere while turning blue as it is oxidized, was added into the system as an indicator (c_{MB} = 6.27 μmol/L). The disappearance of blue represented the depletion of O_2.[31]

RSA Synthesis. Riboflavin (RF), 4-aminosalicylic acid (PAS) and salicylaldehyde (Sal) were used to synthesize the RSA (Figure 1). Thionyl chloride was used as both a solvent and catalyst. PAS and Sal were stirred in thionyl chloride at 30 °C for 12 h with a molar ratio of 1:1. Then RF was added into the mixture in a molar ratio of 1:4.5 with the above-mentioned product. The solvent was dried by air after it was stirred for 24 more hours at 30 °C. The pH of the product was adjusted to 7 with $NaHCO_3$ (solid). Then the product was washed by water and ethanol 3 times respectively and then vacuum filtered. The filter cake was collected and dried in a vacuum at 60 °C. ^1H NMR, mass and FT-IR spectroscopy were used to identify the structure of RSA (Figure S1 and Figure S2, Supporting Information).

Electrodes Preparation. Plain carbon rods, 100 mm in length and 8 mm in diameter, purchased from Jiangsu SuChuang teaching equipment Co., Ltd. (China), were used as the electrode substrates. The anodes were modified by RSA (the average load mass was 5.5 mg) or AQ (the average load mass was 5.2 mg). The carbon rods cleaned by ultrasonication were then immersed in RSA (saturated) or AQ (0.1 g/L) ethanol solution (for 5 min each time) initially. The carbon rods were removed from the solution and dried at 60 °C. The dipping-and-drying process was repeated 20 times (for RSA) and 5 times (for AQ) to increase their loading to achieve a sufficient load mass.

The cathodes were modified by cupric hexacyanoferrate through the interface deposition.[32] The carbon rods cleaned by ultrasonic were then immersed in 0.1 mol/L $K_3[Fe(CN)_6]$ aqueous solution (for 5 min each time) initially. The carbon rods were removed from the solution and dried at 60 °C. Then the carbon rods covered by $K_3[Fe(CN)_6]$ were dipped into 0.2 mol/L $CuCl_2$ ethanol solution (for 10 min each time). Because it has an extremely small solubility in ethanol, $K_3[Fe(CN)_6]$ will react with $CuCl_2$ exceedingly slowly and the cupric hexacyanoferrate will deposit on the surface of carbon rods. Thereby, a compact film was generated after being dried at 60 °C. The dipping-and-drying process was repeated 10 times to increase cupric hexacyanoferrate loading to achieve a sufficient load mass (the average load mass was 565.2 mg). The cathodes were then washed by ultrapure water and dried at 40 °C. All load masses mentioned in the text were detected by adopting gravimetric method.

Surface Characterization. The surface morphologies of RSA modified anode, before and after being used, were examined by a Hitachi SU8010 scanning electron microscope. Briefly, the samples (cut from the anodes) were immersed in 5% (v/v) glutaraldehyde solution for 24 h at 4 °C in order to stabilize the microalgae attached to the anodes. The samples were then rinsed with PBS buffer solution (pH 7.4) for 3 times, dehydrated consecutively with increasing concentration of acetone (50%, 70%, 80%, 90%, 100% and 100% (v/v)) for 20 min each and vacuum freeze-dried.

Measurements and Reagents. The reactor was a transparent common glass sample vial. The individual reaction spaces of reactor were 100 mL. All materials and mediums were sterilized by autoclaving (120 °C, 30 min). The assembled reactor was sealed with epoxy. The anodes of 4 sets of parallel experiments had effective surface areas of 9.57, 9.53, 9.55 and 9.52 cm^2, respectively. The cathodes of 4 sets of parallel experiments had effective surface areas of 9.93, 9.95, 9.58 and 9.99 cm^2, respectively. The distance between the anodes and cathodes was 2 cm. The voltage and current output, cyclic voltammogram were monitored with a polarographic apparatus (797 VA Computrace, Metrohm, Switzerland) and a multimeter (VC97, VICTOR, Xi'an, China). A rheostat (J2361, Feixiang, Jiangsu, China) was employed to measure the internal resistances, polarization and power curves. The COD was determined by colorimetry (DR3900, Hach, Loveland, USA). The CE was calculated by integrating the measured current relative to the theoretical current using the following equation:[27,33]

$$CE = \frac{M\int_0^t I\,dt}{Fbv\Delta COD}$$

DOI: 10.1021/acssuschemeng.5b00151
ACS Sustainable Chem. Eng. 2015, 3, 1974−1981

where v is the volume of chamber of MSC; M = 32, molecular weight of oxygen; F, Faraday's constant = 96 485 C/mol; b = 4, the number of electrons exchanged per mole of oxygen; ΔCOD is the difference in COD at the initial and the end of each separate electricity generation cycles. The concentrations of methyl orange (MO), Orange II, reactive red X-3B (RR) were determined by HPLC (1200, Agilent, Santa Clara, USA, C18 column (5 μm; 150 × 4.6 mm), UV detector (254 nm), the mobile phase (70% methanol, 30% H_2O) was pumped at a rate of 1.0 mL min^{-1}).

All the above-mentioned chemicals were from Sinopharm Chemical Reagent Co., Ltd. (Shanghai, China) and used as received unless otherwise mentioned.

RESULTS AND DISCUSSION

Physicochemical Properties of Redox Mediators. Although riboflavin (log P = −1.097), the substrate of RSA, is often used for biodegradation and MFCs[34] as the RM, it is seldom used for electrode modification due to its poor operability. Compared with RF, which has low solubility (0.012 g) in water, RSA, as a RF derivative, is a compound inclined to hydrophilicity (log P = −0.770) but extremely difficult to dissolve in water. However, its solubility in ethanol (0.027 g) is 2 orders of magnitude higher than that in water (0.000 32 g). This was due to the formation of imine structures (Figure 1), a strong Lewis-base.

As revealed in Figure 2, RSA and RF have similar main redox processes. The same reduction potential of −0.483 V can be found. There were minor differences in oxidation potentials between them (0.02 V). This is because the reaction center of RSA is derived from the active conjugated double bonds of the 1 and 5 position nitrogen atoms on the structure of isoalloxazine, the same as RF. Although the ribityl has no electrochemical activity, the reaction center in the RSA structure is not destroyed. Apart from this, there were slight differences of electrochemical properties between the two materials. Although both of them have the same number of reduction peaks, RSA has only one obvious oxidation peak. Compared with these, RF has another two weaker oxidation peaks (−0.27 and −0.57 V). This is because flavin derivatives can also transfer electrons through the formation of the structure of semiquinone. In addition, the ability of electron gains or losses of 1 and 5 position nitrogen atoms is also different. This is also the reason for the emergence of a number of redox peaks. For RSA, these differences in numbers and the shift of redox peaks might be caused by the structure of imine. As a strong Lewis-base, imine has a strong electron donating ability. It would inhibit the process of electron loss on the structure of isoalloxazine to a certain extent. This also explains why the oxidizability of RSA has been affected to a greater extent than the reducibility.

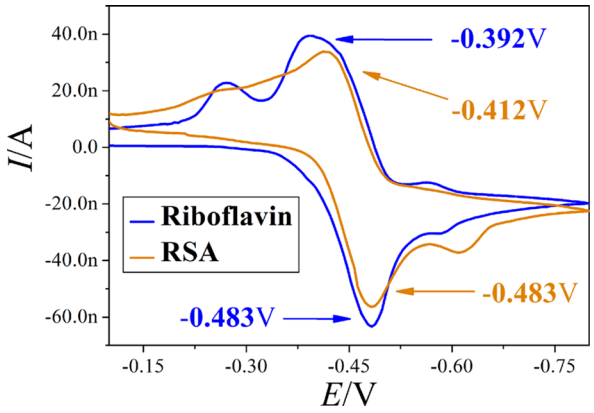

Figure 2. Cyclic voltammogram of riboflavin and RSA (scan rate, 50 mV/s; temperature, 25 °C; working electrode, plain carbon rod; counter electrode, platinum plate; reference electrode, Ag/AgCl-KCl saturated electrode; redox mediator concentration, 1 mg/L; solvent, 0.1 mol/L KNO_3; purged with N_2 for 600 s prior to analysis).

MSCs Performance. Aerating air into the cathode region is commonly used in the traditional single-chamber bioelectrical systems.[35] However, because of the often significant polarization and overpotential of oxygen and requirement of a noble metal catalyst, a conventional air cathode is not efficient and stable enough. Potassium ferricyanide solution is a popular substitute, but it needs to use the membrane.[36] Therefore, cupric hexacyanoferrate, an insoluble compound, was used as a final electron acceptor. It neither occupies device volume nor leads to obvious polarization phenomenon. More importantly, cupric hexacyanoferrate has no toxicity to microorganisms. To evaluate further performance of the MSC after anode was modified, three control experiments were added that contained no RM, used an AQ modified anode or added RF, respectively. Although they have the same microbial growth environment, electrode material and cathode modifications, the electrochemical characteristics of above-mentioned batteries are closely related to the use of RM.

Figure 3 shows that the reactor operated with unmodified anode reached a steady open circuit voltage (OCV) of 0.57 V, which was significantly lower than that of the reactor operated with the RSA modified anode (0.81 V) and RF added (0.78 V). The OCV of the AQ modified system was only 0.03 V higher than the reactor operated without RM. The cathode potentials offered by cupric hexacyanoferrate were 0.36 V.[33] Although there was no liquid junction potential, this potential was almost not lost in the homogeneous (solid phase) reaction. The anode potential is dependent on the oxidation potential of the electron donor. This value was −0.30 V in the unmodified anode system in which acetate was used as the carbon source.[33] There was a significant loss of cell potential (0.24 V on OCV) in the RM-free system. It can be observed that there was minimum substrate conversion efficiency (reduced by 86.9% on power density) in this system. The growth of microorganisms can set up thermodynamic potentials in terms of substrates, pH and other gradients that can often lead to the generation of an electromotive force, but not to appreciable current generation. It can be predicted that the loss of cell voltage of RM-free system would be more obvious when the load was added (There will no longer be concentration potential).[37] RSA and

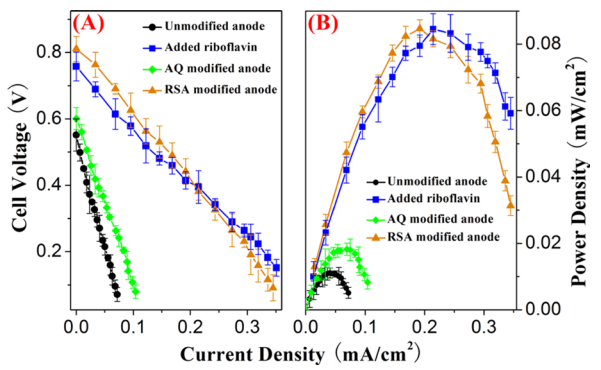

Figure 3. Power density curves and polarization curves of MSCs.

DOI: 10.1021/acssuschemeng.5b00151
ACS Sustainable Chem. Eng. 2015, 3, 1974−1981

RF have much higher oxidation potentials (−0.412 and −0.392 V, respectively) than acetate. The system containing RF can greatly accelerate the rate of consumption of acetate, which to some extent made up for the disadvantage of low efficiency of electron transport on the surface of electrodes. Meanwhile, the electrons from the oxidation state RF were partly captured by the anode, which made the OCV of system containing RF reach up to 0.78 V. For the system using the RSA modified anode, the electrons through which the anode was obtained were totally received from the oxidation state RSA. The anode potential was almost not lost. The polarization curve of anode modified system had a greater slope than that of the RF added system. This is because the anode modified system produced far fewer electrons than that of system containing RF. Surprisingly, AQ (log P = 3.400) was extremely unlikely to enhance performance of the MSC as an insoluble RM. In contrast with RSA, AQ has almost no effect on OCV of MSC though it has an oxidation potential of about −0.25 V.[38] This property was quite different from its soluble derivatives such as anthraquinone-2,6-disulfonic disodium salt (log P = 0.400).[39] It can be seen that solubility is not the only factor that affects the performance of electron transfer.

As shown in Figure 3, the current densities and power densities of a system containing RF or RSA were much higher than those of a nonmediator or AQ-contained system. As a result of homogeneous catalysis, despite the fact that it had low anode surface electron transfer efficiency, a system containing RF still had the power density of 0.845 W/m^2. This might be due to the rapid consumption of electron donors (the reaction rate was 0.79 mmol·L^{-1}·h^{-1}, to sodium acetate meter). Although the system using the RSA modified anode had only nearly one-third of the acetate consumption rate (0.29 mmol·L^{-1}·h^{-1}) of the system containing RF, it had a greater electron utilization rate (CE = 14.1%). This would compensate for the above-mentioned shortcoming. When the anode modified systems was up to the maximum power density of 0.847 W/m^2, it had a lower current density than that of the system contained RF. In fact, the differences of operating voltage and the OCV among the three systems were not enormous. The state of reactants determined the internal resistances of those systems and thus determined the current densities indirectly. There is no denying that the power density of this MSC is lower than other power generation systems using light such as silicon solar cells and dye sensitized solar cells or traditional bacteria-based MFCs. But this system still improved the performance of similar algae-based MSCs by about 2 times.[40,41] Substrates in no mediator system were in a state of difficult ionization. The corresponding power density was as low as 0.111 W/m^2. This was another example that the electron transport efficiency on the surface of electrodes was also an important determinant of internal resistances of MSCs. Once again, AQ failed to improve significantly the power output of MSC (0.185 W/m^2). It can initially be inferred that electrostatic interaction is the key factor that might affect the electron transfer.

Besides, the cupric hexacyanoferrate modified cathode was indeed almost completely eliminated polarization. These differences are reflected in Figure 4. The OCVs of unmodified cathode controls were all decreased by about 0.1 V. Not only that, the operating voltages of unmodified cathode controls rapidly dropped by an average of 60%. Then their current densities and power densities were also to drop inevitably. These data were also reduced by two-thirds. There was no

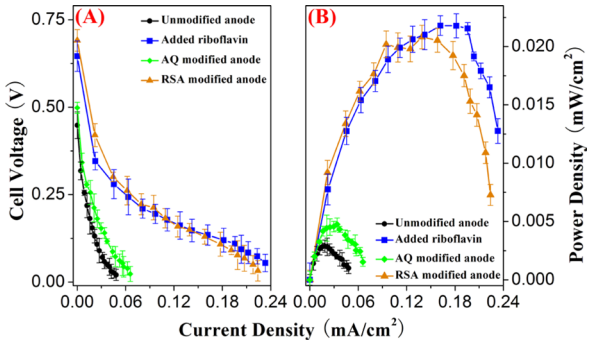

Figure 4. Power density curves and polarization curves of the corresponding MSCs with unmodified cathodes.

doubt that the linearity of their polarization curves was also decreased significantly. These fully showed that cupric hexacyanoferrate had similar positive impacts on the above-mentioned systems.

To investigate further the performance of the above-mentioned systems, a continuous observation of their operating voltages and electricity generation cycles was conducted. Because of the consumption of sodium acetate by *C. vulgaris*, the cell voltages would drop over time. When their cell voltages dropped to a maximum operating voltage of 10%, the battery was considered to have completed one cycle of electricity generation. At this point, sodium acetate was added to corresponding reactors to make their concentration reach 0.02 mol/L. The cathode would also be replaced at the same moment (although there was very little (the final average consumption of cupric hexacyanoferrate was 49.4 mg). For RSA, AQ and RF, they would no longer be supplemented. Because each system had different start-up periods, their complete electricity generation cycles in 240 h were selected for analysis. Figure 5 shows the hydrophilic RMs indeed can

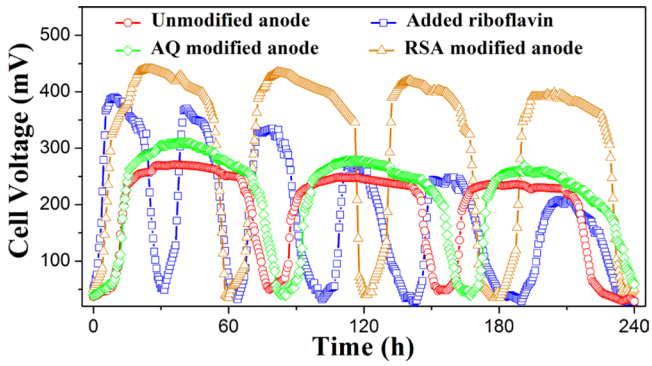

Figure 5. Power output curves of MSCs. Cell voltage as a function of time with external resistances of 500 Ω (unmodified), 500 Ω (AQ modified), 100 Ω (RSA modified) and 100 Ω (added RF), respectively. RF concentration, 10 mg/L.

significantly accelerate the consumption rates of acetate by *C. vulgaris*. The system adding RF included 6 complete electricity generation cycles in 12 days. This value was 4 for the RSA modified system in the same conditions. The mediator-free system contained only 3 electricity production cycles in the same period. Compared with the nonmediator system, the average single electricity generation cycles of systems adding RF and using RSA modified anode were respectively shortened to 50% and 75%. Similar to the OCV, AQ also had a minimal

DOI: 10.1021/acssuschemeng.5b00151
ACS Sustainable Chem. Eng. 2015, 3, 1974−1981

Table 1. Comparison of Open Circuit Voltage (OCV), Power Density (PD), COD Removal Efficiency (η_{COD}), Coulombic Efficiency (CE), Start-up Period and Voltage Loss for Different Systems[a]

system	OCV (V)	PD (W/m^2)	η_{COD} (%)	CE (%)	start-up period (h)	voltage loss (%)
unmodified anode	0.57 ± 0.03	0.111 ± 0.012	90.7 ± 3.3	10.0 ± 0.3	120	11.5 ± 0.6
AQ modified anode	0.60 ± 0.03	0.185 ± 0.015	92.7 ± 3.9	10.6 ± 0.4	92	12.9 ± 0.8
added riboflavin	0.78 ± 0.04	0.845 ± 0.041	95.5 ± 1.1	5.1 ± 0.1	44	50.0 ± 3.3
RSA modified anode	0.81 ± 0.04	0.847 ± 0.024	94.6 ± 1.8	14.1 ± 0.7	29	9.1 ± 0.6

[a]Error values represent standard deviations of replicate samples.

impact on the power output of MSC. Indeed, although a slight increase was observed in power output, there was also an increase of 10% in the length of single electricity generation cycle. It illustrated that it was difficult for the hydrophobic catalytic to have a positive impact on electron transfer in aqueous phase.

More importantly, the integrated area of a single cycle can approximately reflect the CE of each system. As can be seen from the Table 1, although the system containing RF had the shortest reaction period, it had the lowest CE of 5.1% (first electricity generation cycle, same as below). Because the reaction rate was too high, the resultants had no time to reach the surface of electrodes through the free diffusion. Although a high internal resistance reduced its power output and there was no RM in reactor, the nonmediator system had a higher CE of 10.0% than the system containing RF. This value was 10.6% for the AQ modified system on average. The anode modified system, also in the case of absence of soluble RM, had the highest CE up to 14.1%. When MSCs completed one cycle of electricity generation, their COD removal efficiencies were exceeded by 90%. Even if it was a heterogeneous catalysis, RSA still greatly accelerated the rates of reactions in solution. This indicated that the electron transfer efficiency was certainly an important factor that affected the CE, but the solid phase catalysts on the surface of electrodes can also affect the liquid phase reactions. It can be inferred that the RSA on the surface of anode formed a film of single-molecule hydration layer. The hydrated RSA molecular was easily combined with free electrons in solution and then reduced. The reduction state RSA which was negatively charged would exchange with the oxidation state RSA and then release electrons on surface of carbon rod. The oxidation state RSA spread to hydration layer would repeat this process. Although it might also have the same properties, the degree of hydration of AQ was inevitably low. That is to say, there was very weak electrostatic interaction between AQ and hydrated anions.

Although the use of RF made the system get a high initial operating voltage and power density, the loss of operating voltage was very significant. The operating voltage dropped even less than the nonmediator system after about 200 h. The voltage loss was up to 50%. The consequent increase in internal resistance led to further decline in power density. For the system adding RF, another important change was the growth of length of single electricity generation cycle. The last cycle was nearly 2 times the length of the first one. All of these proved that RF was depleted rapidly. This is also the disadvantage of all soluble RMs. In contrast, the operating voltage of the anode modified system was almost unchanged throughout the whole reaction process. The length of each cycle had no significant change. This was almost identical with the nonmediators and the AQ-contained system (the final average load mass was 5.0 mg). Both of them lost only 10% of operating voltage. In other words, little if anything of RSA (the final average load mass was 5.5 mg) was consumed under such conditions. RSA in aqueous phase did have the tendency of hydrolysis and photolysis as an ester and a photosensitive compound. Stable power output was sufficient to explain the stability of RSA under experimental environment. It showed that the hydrophobically modified not only increased the lipophilic of RSA so that it could not use any carrier to be attached to the surface of plain carbon rod, but also improved its stability in aqueous solutions indirectly. Thus, there was a sharp decline in degree of hydrolysis. Further, as it was difficult to go into aqueous solutions, the light stability of RSA was also substantially increased. Moreover, the life cycle of *C. vulgaris* was longer than the experimental time. The above influential factors can almost be ignored. Because the cathodes used in every separate cycle were new, it can be certain that the react conditions in above systems were equal. Obviously, the RM was the main factor which affected the potential and power densities. In addition, a slowly voltage drop occurred in each separate electricity generation cycles of RM contained systems. This displayed the nonlinear consumption of substrates. Thus, the catalytic efficiency was related to substrate consumption rate.

Anyway, the use of RSA modified anode improved the performance of original system greatly. The operating voltage (0.44 V), conductance (0.01 S), power density (0.847 W/m^2), reaction rate (0.29 mmol·L^{-1}·h^{-1}, to sodium acetate meter) and CE (14.1%) were increased by 63%, 367%, 663%, 74% and 41%, respectively. These were close to or even exceeded what RF-contained system exhibited. What is more, purely hydrophobic modification might reduce the efficiency of microbial reactions performed in aqueous phase. Though RSA is insoluble in water, its octanol−water partition coefficient (log P = −0.770) also explained why it had a strong catalytic effect on the reactions in aqueous phase.

Characteristics of Surface Catalysis. To verify further that hydrophilicity was one of the important factors to determine the catalytic performance of the anodes, a group of control experiments of decolorization was conducted. Three structurally similar compounds, MO, OrangeII and RR, which all contains azo bonds, were used to evaluate the performance of dye removal efficiency in the above-mentioned MSCs. Similar to the RMs, although the reaction conditions and chromophore were the same, the rates of decolorization still depended more on the hydrophilicity of azo dyes. As shown in Figure 6, the rate of decolorization of RR (log P = −1.865) was far more than that of OrangeII (log P = −0.408) and MO (log P = 0.415) in any conditions. The decolorization rate promoted by AQ was rather little by comparing their half-lives. It can be seen that hydrophobic compounds in aqueous solution did have very weak electrostatic and hydrogen bonding interaction with hydrophilic compounds. As shown in Figure 6A, in the case of the same concentration of MO (5×10^{-4} mol/L), the half-life of the RM-free system was 3.866 h. By contrast, RSA modified system consumed 3.118h to achieve this effect. This

DOI: 10.1021/acssuschemeng.5b00151
ACS Sustainable Chem. Eng. 2015, 3, 1974−1981

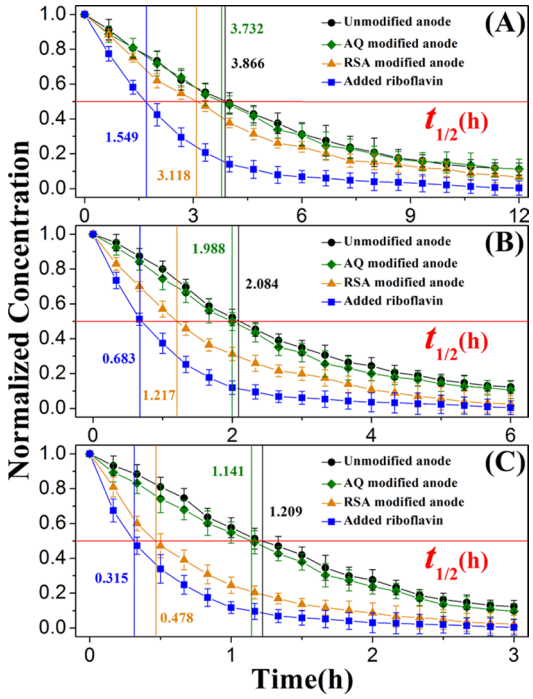

Figure 6. Time profiles of normalized concentration of azo dyes. (A) MO, (B) OrangeII, (C) RR. Dye concentration, 5×10^{-4} mol/L.

value was only 1.549 h in the system added RF. The half-lives of OrangeII were 2.804 h (RM-free), 1.988 h (contained AQ), 1.217 h (contained RSA) and 0.683 h (contained RF) correspondingly. For RR, it consumed only 1.209 h (RM-free), 1.141 h (contained AQ), 0.478 h (contained RSA) and 0.315 h (contained RF), respectively, to achieve the same effect. Even in homogeneous catalysis, RF had a better enhancement effect on more hydrophilic dyes. The half-lives of decolorization of MO, OrangeII and RR were shortened by 149.6%, 205.1% and 283.8%, respectively. For heterogeneous catalysis, RSA still shortened the half-lives of decolorization of above-mentioned azo dyes by 24.0%, 71.2% and 153.0%, respectively. This trend was consistent with the RF. The stronger the hydrophilic of dyes, the smaller the gap between the promotion rates of RF and RSA. As a matter of fact, although the promotion rates were very low, AQ, a hydrophobic RM, was still consistent with this rule in aqueous solution. This fully illustrated that hydrophilic catalysis did have a greater capacity of capturing hydrated anions under such conditions.

SEM Study. Although the RSA modified anode significantly increased the performance of the system, there was still the possibility that this improvement might be due to the enhancement of biocompatibility of the anode surface rather than the promotion of electron transfer efficiency. To prove this, we conducted a study of SEM of the anode we used before and after the experiment. As shown in Figure 7, there were no obvious changes in the surface morphology of anodes modified with RSA (Figure 7b-1) or not (Figure 7a-1), indicating that RSA cannot form regular crystal but uniformly adheres to carbon rod in amorphous state. The modification was harmless to the carbon rod itself. By comparison, although the surfaces of

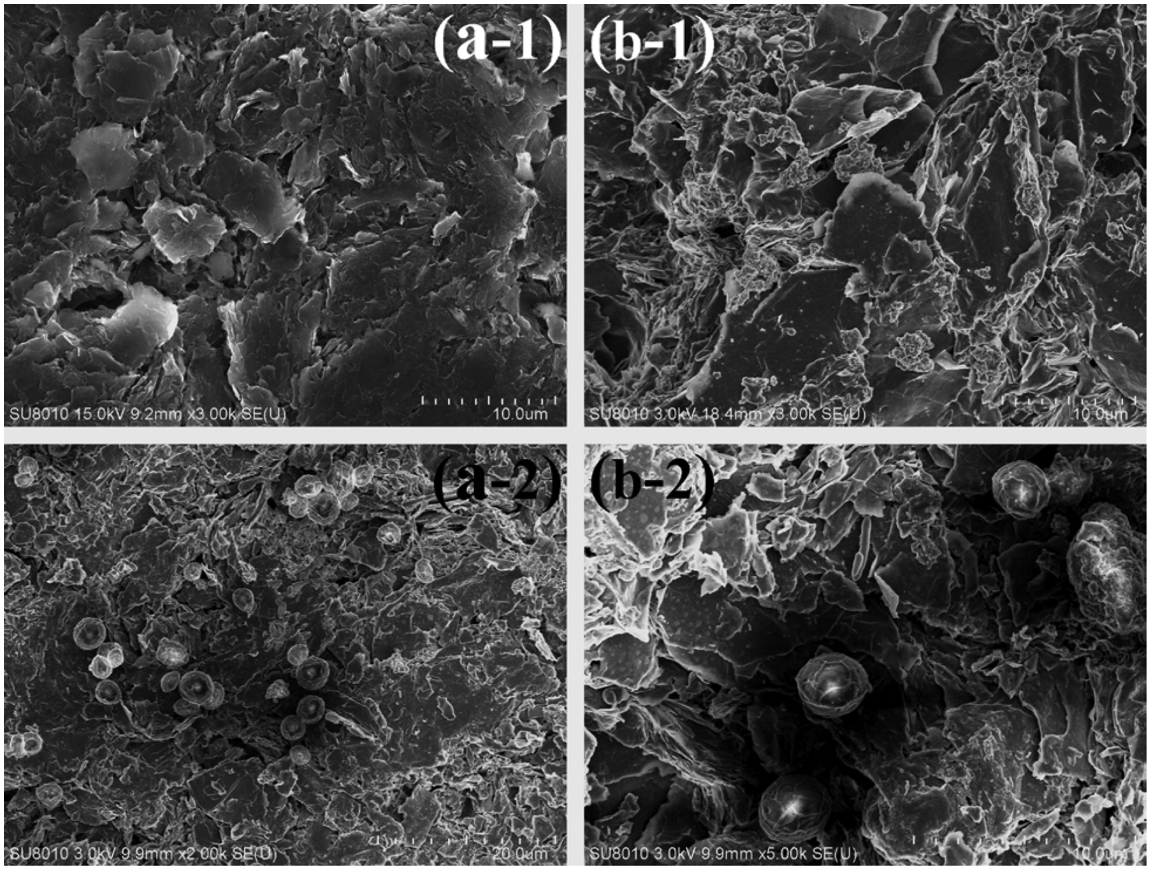

Figure 7. SEM images of (a-1) as-received unmodified carbon rod, (a-2) used unmodified carbon rod attached with *C. vulgaris*, (b-1) as-prepared RSA modified carbon rod, (b-2) used RSA modified carbon rod attached with *C. vulgaris*.

DOI: 10.1021/acssuschemeng.5b00151
ACS Sustainable Chem. Eng. 2015, 3, 1974−1981

the used anodes (Figure 7a-2,b-2) showed slight erosions and some visible impurities adhered, there were still no significant changes in the surface morphology. More evident was that because a little scattered *C. vulgaris* were attached to both anodes, they could not form a stable biofilm. This fully illustrated that hydrophilic modification was not conducive to microbial attachment. Besides, the *C. vulgaris* cell wall itself is a poor conductor. The acceleration of electron transfer process in this study was indeed caused by modifications of the anode but not through *C. vulgaris* itself.

Additionally, cupric hexacyanoferrate was nonrenewable under normal conditions. To this end, a simple way was used to solve this problem. Because the original system was run anaerobically, the *C. vulgaris* was mainly responsible for photofermentation at the initial growth stage. By adjusting the illumination intensity (500 lx) of the cathode region, the *C. vulgaris* within this area would keep a low respiratory O_2 consumption rate. The *C. vulgaris* mainly carried photosynthesis. Through this way, *C. vulgaris* would be able to carry out different types of metabolisms in the same space without a separator. The cupric hexacyanoferrate was reduced to cupric ferrocyanide by electrons generated from anode reactions. The O_2 produced by photosynthesis was reacted with cupric ferrocyanide and H_2O to generate Fe^{3+} and OH^-. The Fe^{3+} would regenerate to cupric hexacyanoferrate and redeposit on the surface of the cathode. MB was also added into the system as an indicator. Thus, the regions of different types of metabolisms were clearly indicated (Figure S3, Supporting Information).[31]

CONCLUSION

In summary, the excellent capability of capturing free electrons in solution of RSA was demonstrated. Although there were microorganisms scarcely attached to the surface of the anode, the OCV and power densities were increased by 41% and 663%, respectively, compared with the original system. With the improvement of reaction efficiency, the electricity generation period was shortened by 25%. Because the RSA itself was modified through the incorporation of hydrophobic groups rather than embedded in the carrier, this method was more inexpensive, quicker and easier. The characteristics of almost no loss of RSA in the course of reaction would also greatly increase the life of the anode. This promising method provides the possibility of enhancing its performance of current generation greatly and also shortens the start-up period significantly. The enhancement of electron capture capability provides a convenient way to construct renewable biocathode by light autotrophic microorganisms. The current studies are significant in that they can be further extended to other algae-based microbial solar cells.

ASSOCIATED CONTENT

Supporting Information

The Supporting Information is available free of charge on the ACS Publications website at DOI: 10.1021/acssuschemeng.5b00151.

Further detailed information about ^1H NMR and mass spectroscopy of RSA. FT-IR spectroscopy of RF, SA and RSA. Photo of the constructed microbial solar cell (PDF).

AUTHOR INFORMATION

Corresponding Author

*P. Zhou. Fax: +86-27-68778893. Tel: +86-27-87152823. E-mail: zhoupj@whu.edu.cn.

Notes

The authors declare no competing financial interest.

ACKNOWLEDGMENTS

This study was supported by the Open Fund of Hubei Biomass-Resource Chemistry and Environmental Biotechnology Key Laboratory (HBRCEBL2011-2012005) and the Fundamental Research Funds for the Central Universities (No. 2012205020210).

REFERENCES

(1) Sakimoto, K. K.; Liu, C.; Lim, J.; Yang, P. Salt-induced self-assembly of bacteria on nanowire arrays. *Nano Lett.* **2014**, *14* (9), 5471−6.

(2) Wang, Y.; Li, B.; Cui, D.; Xiang, X.; Li, W. Nano-molybdenum carbide/carbon nanotubes composite as bifunctional anode catalyst for high-performance Escherichia coli-based microbial fuel cell. *Biosens. Bioelectron.* **2014**, *51*, 349−55.

(3) Liu, B.; Brückner, C.; Lei, Y.; Cheng, Y.; Santoro, C.; Li, B. Cobalt porphyrin-based material as methanol tolerant cathode in single chamber microbial fuel cells (SCMFCs). *J. Power Sources* **2014**, *257*, 246−253.

(4) Zhao, F.; Harnisch, F.; Schröder, U.; Scholz, F.; Bogdanoff, P.; Herrmann, I. Application of pyrolysed iron(II) phthalocyanine and CoTMPP based oxygen reduction catalysts as cathode materials in microbial fuel cells. *Electrochem. Commun.* **2005**, *7* (12), 1405−1410.

(5) Feng, C.; Ma, L.; Li, F.; Mai, H.; Lang, X.; Fan, S. A polypyrrole/anthraquinone-2,6-disulphonic disodium salt (PPy/AQDS)-modified anode to improve performance of microbial fuel cells. *Biosens. Bioelectron.* **2010**, *25* (6), 1516−20.

(6) Zhu, N.; Chen, X.; Zhang, T.; Wu, P.; Li, P.; Wu, J. Improved performance of membrane free single-chamber air-cathode microbial fuel cells with nitric acid and ethylenediamine surface modified activated carbon fiber felt anodes. *Bioresour. Technol.* **2011**, *102* (1), 422−6.

(7) Xia, X.; Zhang, F.; Zhang, X.; Liang, P.; Huang, X.; Logan, B. E. Use of pyrolyzed iron ethylenediaminetetraacetic acid modified activated carbon as air-cathode catalyst in microbial fuel cells. *ACS Appl. Mater. Interfaces* **2013**, *5* (16), 7862−6.

(8) Ma, M.; Dai, Y.; Zou, J. L.; Wang, L.; Pan, K.; Fu, H. G. Synthesis of iron oxide/partly graphitized carbon composites as a high-efficiency and low-cost cathode catalyst for microbial fuel cells. *ACS Appl. Mater. Interfaces* **2014**, *6* (16), 13438−47.

(9) Liu, W.; Mu, W.; Liu, M.; Zhang, X.; Cai, H.; Deng, Y. Solar-induced direct biomass-to-electricity hybrid fuel cell using polyoxometalates as photocatalyst and charge carrier. *Nat. Commun.* **2014**, *5*, 3208.

(10) Zhang, Y.; Hu, Y.; Li, S.; Sun, J.; Hou, B. Manganese dioxide-coated carbon nanotubes as an improved cathodic catalyst for oxygen reduction in a microbial fuel cell. *J. Power Sources* **2011**, *196* (22), 9284−9289.

(11) Forrestal, C.; Huang, Z.; Ren, Z. J. Percarbonate as a naturally buffering catholyte for microbial fuel cells. *Bioresour. Technol.* **2014**, *172*, 429−32.

(12) Wei, L.; Han, H.; Shen, J. Effects of cathodic electron acceptors and potassium ferricyanide concentrations on the performance of microbial fuel cell. *Int. J. Hydrogen Energy* **2012**, *37* (17), 12980−12986.

(13) Niu, C. G.; Wang, Y.; Zhang, X. G.; Zeng, G. M.; Huang, D. W.; Ruan, M.; Li, X. W. Decolorization of an azo dye Orange G in microbial fuel cells using Fe(II)-EDTA catalyzed persulfate. *Bioresour. Technol.* **2012**, *126*, 101−6.

DOI: 10.1021/acssuschemeng.5b00151
ACS Sustainable Chem. Eng. 2015, 3, 1974−1981

(14) Chen, H.; Zheng, P.; Zhang, J.; Xie, Z.; Ji, J.; Ghulam, A. Substrates and pathway of electricity generation in a nitrification-based microbial fuel cell. *Bioresour. Technol.* **2014**, *161*, 208−14.
(15) Wang, Y.; Li, B.; Zeng, L.; Cui, D.; Xiang, X.; Li, W. Polyaniline/mesoporous tungsten trioxide composite as anode electrocatalyst for high-performance microbial fuel cells. *Biosens. Bioelectron.* **2013**, *41*, 582−8.
(16) Adachi, M.; Shimomura, T.; Komatsu, M.; Yakuwa, H.; Miya, A. A novel mediator-polymer-modified anode for microbial fuel cells. *Chem. Commun. (Cambridge, U. K.)* **2008**, *17*, 2055−7.
(17) Santoro, C.; Guilizzoni, M.; Correa Baena, J. P.; Pasaogullari, U.; Casalegno, A.; Li, B.; Babanova, S.; Artyushkova, K.; Atanassov, P. The effects of carbon electrode surface properties on bacteria attachment and start up time of microbial fuel cells. *Carbon* **2014**, *67*, 128−139.
(18) Sun, M.; Reible, D. D.; Lowry, G. V.; Gregory, K. B. Effect of applied voltage, initial concentration, and natural organic matter on sequential reduction/oxidation of nitrobenzene by graphite electrodes. *Environ. Sci. Technol.* **2012**, *46* (11), 6174−81.
(19) Zhao, H.; Zhang, Y.; Zhao, B.; Chang, Y.; Li, Z. Electrochemical reduction of carbon dioxide in an MFC-MEC system with a layer-by-layer self-assembly carbon nanotube/cobalt phthalocyanine modified electrode. *Environ. Sci. Technol.* **2012**, *46* (9), 5198−204.
(20) Gnana kumar, G.; Kirubaharan, C. J.; Udhayakumar, S.; Ramachandran, K.; Karthikeyan, C.; Renganathan, R.; Nahm, K. S. Synthesis, Structural, and Morphological Characterizations of Reduced Graphene Oxide-Supported Polypyrrole Anode Catalysts for Improved Microbial Fuel Cell Performances. *ACS Sustainable Chem. Eng.* **2014**, *2* (10), 2283−2290.
(21) Rosenbaum, M.; Zhao, F.; Schroder, U.; Scholz, F. Interfacing electrocatalysis and biocatalysis with tungsten carbide: a high-performance, noble-metal-free microbial fuel cell. *Angew. Chem., Int. Ed.* **2006**, *45* (40), 6658−61.
(22) Yuan, Y.; Zhou, S.; Liu, Y.; Tang, J. Nanostructured macroporous bioanode based on polyaniline-modified natural loofah sponge for high-performance microbial fuel cells. *Environ. Sci. Technol.* **2013**, *47* (24), 14525−32.
(23) Alvarez, L. H.; Perez-Cruz, M. A.; Rangel-Mendez, J. R.; Cervantes, F. J. Immobilized redox mediator on metal-oxides nanoparticles and its catalytic effect in a reductive decolorization process. *J. Hazard. Mater.* **2010**, *184* (1−3), 268−72.
(24) Zhang, P.; Xu, D.; Li, Y.; Yang, K.; Gu, T. Electron mediators accelerate the microbiologically influenced corrosion of 304 stainless steel by the Desulfovibrio vulgaris biofilm. *Bioelectrochemistry* **2015**, *101*, 14−21.
(25) Liu, M.; Yuan, Y.; Zhang, L. X.; Zhuang, L.; Zhou, S. G.; Ni, J. R. Bioelectricity generation by a Gram-positive Corynebacterium sp. strain MFC03 under alkaline condition in microbial fuel cells. *Bioresour. Technol.* **2010**, *101* (6), 1807−11.
(26) Habermann, W.; Pommer, E. H. Biological fuel cells with sulphide storage capacity. *Appl. Microbiol. Biotechnol.* **1991**, *35*, 128−33.
(27) Rabaey, K.; Verstraete, W. Microbial fuel cells: novel biotechnology for energy generation. *Trends Biotechnol.* **2005**, *23* (6), 291−8.
(28) Harnisch, F.; Schroder, U. From MFC to MXC: chemical and biological cathodes and their potential for microbial bioelectrochemical systems. *Chem. Soc. Rev.* **2010**, *39* (11), 4433−48.
(29) Darus, L.; Ledezma, P.; Keller, J.; Freguia, S. Oxygen suppresses light-driven anodic current generation by a mixed phototrophic culture. *Environ. Sci. Technol.* **2014**, *48* (23), 14000−6.
(30) Winkler, M.; Hemschemeier, A.; Gotor, C.; Melis, A.; Happe, T. [Fe]-hydrogenases in green algae photo-fermentation and hydrogen evolution under sulfur deprivation. *Int. J. Hydrogen Energy* **2002**, *27*, 1431−39.
(31) Pan, K.; Zhou, P. A hermetic self-sustained microbial solar cell based on Chlorella vulgaris and a versatile charge transfer chain. *J. Power Sources* **2015**, *293* (0), 467−474.
(32) Chen, X.; Xie, H.; Seow, Z. Y.; Gao, Z. An ultrasensitive DNA biosensor based on enzyme-catalyzed deposition of cupric hexacyanoferrate nanoparticles. *Biosens. Bioelectron.* **2010**, *25* (6), 1420−1426.
(33) Logan, B. E.; Regan, J. M. Electricity-producing bacterial communities in microbial fuel cells. *Trends Microbiol.* **2006**, *14* (12), 512−8.
(34) Yong, Y. C.; Cai, Z.; Yu, Y. Y.; Chen, P.; Jiang, R.; Cao, B.; Sun, J. Z.; Wang, J. Y.; Song, H. Increase of riboflavin biosynthesis underlies enhancement of extracellular electron transfer of Shewanella in alkaline microbial fuel cells. *Bioresour. Technol.* **2013**, *130*, 763−8.
(35) Zhang, X.; Xia, X.; Ivanov, I.; Huang, X.; Logan, B. E. Enhanced activated carbon cathode performance for microbial fuel cell by blending carbon black. *Environ. Sci. Technol.* **2014**, *48* (3), 2075−81.
(36) Liao, Q.; Zhang, J.; Li, J.; Ye, D.; Zhu, X.; Zhang, B. Increased performance of a tubular microbial fuel cell with a rotating carbon-brush anode. *Biosens. Bioelectron.* **2015**, *63*, 558−61.
(37) Logan, B. E. Essential data and techniques for conducting microbial fuel cell and other types of bioelectrochemical system experiments. *ChemSusChem* **2012**, *5* (6), 988−94.
(38) Guo, J.; Liu, H.; Qu, J.; Lian, J.; Zhao, L.; Jefferson, W.; Yang, J. The structure activity relationship of non-dissolved redox mediators during azo dye bio-decolorization processes. *Bioresour. Technol.* **2012**, *112*, 350−4.
(39) Sun, J.; Li, W.; Li, Y.; Hu, Y.; Zhang, Y. Redox mediator enhanced simultaneous decolorization of azo dye and bioelectricity generation in air-cathode microbial fuel cell. *Bioresour. Technol.* **2013**, *142*, 407−14.
(40) Venkata Mohan, S.; Srikanth, S.; Chiranjeevi, P.; Arora, S.; Chandra, R. Algal biocathode for in situ terminal electron acceptor (TEA) production: Synergetic association of bacteria-microalgae metabolism for the functioning of biofuel cell. *Bioresour. Technol.* **2014**, *166*, 566−74.
(41) González del Campo, A.; Cañizares, P.; Rodrigo, M. A.; Fernández, F. J.; Lobato, J. Microbial fuel cell with an algae-assisted cathode: A preliminary assessment. *J. Power Sources* **2013**, *242*, 638−645.

DOI: 10.1021/acssuschemeng.5b00151
ACS Sustainable Chem. Eng. 2015, 3, 1974−1981